

# Does the Iron $K_\alpha$ Line of Active Galactic Nuclei Arise from Cerenkov Line-like Radiation?

*J. H. You<sup>1,2</sup>, D. B. Liu<sup>1</sup>, W. P. Chen<sup>3</sup>, L. Chen<sup>1</sup>, S. N. Zhang<sup>4</sup>*

<sup>1</sup>*Institute for Space and Astrophysics, Department of Physics, Shanghai Jiao-Tong University, Shanghai, 200030, China, P. R.*

<sup>2</sup>*jhyou@online.sh.cn*

<sup>3</sup>*Institute of Astronomy and Department of Physics, National Central University, Chung-Li, 32054, Taiwan, China*

<sup>4</sup>*Center for Astrophysics, Physics Department, Tsinghua University, Beijing, 100084, China, P. R.*

## ABSTRACT

When thermal relativistic electrons move through a gas region, or impinge upon the surface of a cloud that consists of a dense gas or doped dusts, the Cerenkov effect produces a peculiar atomic or ionic emission line—the Cerenkov line-like radiation. This newly recognized emission mechanism may find wide applications in high-energy astrophysics. We propose that the Cerenkov process may be a mechanism to compete with the fluorescence emission to account for the broad, asymmetric, and elusively variable  $K_\alpha$  line at  $\sim 6.4\text{--}6.5$  KeV detected in some of the Seyfert 1 galaxies. We argue that some observations that do not lend direct support to the fluorescence model, for example an apparent lack of a temporal response of the Fe line flux to the changes of the X-ray continuum flux, or the lack of a *prominent* K-absorption edge of iron ions around  $\sim 7\text{--}8$  KeV, may be readily reconciled with the Cerenkov process. If the Cerenkov line radiation is indeed responsible significantly for the Fe  $K_\alpha$  emission, the conventional scenario around the central supermassive black holes of AGNs would need to be drastically modified to accommodate more energetic, more violent and much denser environments than previously thought.

## 1. Iron $K_\alpha$ Emission Line around Black Holes

Observations in the last decade show that many active galactic nuclei (AGNs), e.g., the Seyfert 1 galaxies, show an emission feature peaked around  $\sim 6.4\text{--}6.5$ KeV, commonly attributed to  $K_\alpha$  line of iron ions in low- or intermediate-ionization states. The observed  $K_\alpha$  line is very broad, and the line profile is asymmetric, being steep on the blue and flattening on the red wavelength wing, extending to  $4\text{--}5$ KeV, as shown in Fig. 1 (Tanaka et al. 1995; Nandra et al. 1997, 1997b; Fabian et al. 2002; Gordin et al. 2001). The iron  $K_\alpha$  is regarded as one of the best probes to explore the physical mystery in regions proximate to the central supermassive black

holes of AGNs. Its observation and interpretation thus have drawn great attention lately in black hole and AGN study.

The prevailing “reflection disk-fluorescence line” model (e.g., Guilbert et al. 1998; Lightman et al. 1998; Fabian et al. 1989; Reynolds 2001) for the observed low-ionization Fe  $K_\alpha$  line in AGNs calls for a supermassive black hole harbored at the center of an AGN, which accretes significant amounts of material from the surrounding host galaxy. The angular momentum of the incoming material leads to the formation of a flattened rotating accretion disk of a cold gas. Here “cold” means that the maximum temperature in the innermost region of the disk near the central black hole is only  $T \sim 10^5 - 10^6$  K. Most of the metal atoms, including iron, are therefore in low- or intermediate-ionization states, while hydrogen and helium are nearly fully ionized. Sandwiching the accretion disk is a hot and tenuous corona from which copious hard X-ray continuum with a power-law spectrum originates. Strong irradiation of the hard X rays causes an ionization layer at the surface of the disk off which subsequent, incident X-ray photons will be scattered by free or bound electrons and reflected back to the corona, forming a reflection continuum. Part of the incident X-ray photons may get to penetrate into the cold disk and subject to photoionization (photoelectric) absorption by heavy ions. Fluorescence line emission follows, among which the strongest is the iron  $K_\alpha$  line, produced by transition  $n = 2 \rightarrow 1$  when one of the 2 K-shell (the ground state) electrons is ejected out due to the photoelectric absorption of an X-ray photon with energy  $h\nu \gtrsim 7 - 8$  KeV, higher than the ionization threshold of the K-shell of iron ion in low or intermediate ionization.

If fluorescent line photons are produced in the inner part of the rotating disk, a broadened and red-asymmetric line profile results, as what has been observed for the Fe  $K_\alpha$  line, due to both the special relativistic (Doppler broadening /boosting) and general relativistic (gravitational redshift) effects. With the “disk-line” model, Tanaka et al.(1995) successfully explained the Fe  $K_\alpha$  line profile of the Seyfert 1 galaxy MCG–6–30–15. The model has gained wide popularity because it produces line profile consistent with observations. Furthermore, the underlying emission mechanism, that is, photoelectric absorption followed by fluorescence line emission, has been so far taken for granted as the only way to produce the X-ray line emission of heavy atoms or ions in low- or intermediate-ionization states. Taking an iron ion as an example, because the K-shell is fully closed, the transition  $n = 2 \rightarrow 1$  ( $K_\alpha$ ) cannot occur unless certain external X-ray illumination causes photoelectric absorption to first make a “vacancy” in the K-shell.

## 2. Difficulties Confronting Observations

Despite the success in producing the observed line profile, however, the photoelectric absorption-fluorescence mechanism has two consequences that fail to reconcile with currently available observations. First, there should have been a temporal response of the Fe line flux to the changes of the X-ray continuum in the fluorescence process. Rapid variabilities of X rays are observed in most AGNs. With the fluorescence mechanism, the Fe  $K_\alpha$  line flux should follow the

changes of the incident X rays. However, as observed in either MCG–6–30–15 or NGC 5548, the Fe  $K_\alpha$  flux remained nearly constant, despite the rapid variations of the X-ray continuum (Lee et al. 1999, 2000; Chiang et al. 2000); no response to the incident X rays was observed. It has been suggested that a flux-correlated change of ionization states of the iron element might be responsible for the lack of correlation between the fluxes of Fe  $K_\alpha$  line and the continuum (e.g., Reynolds 2001). But so far no quantitative analysis has been done to support this viewpoint. Besides, recent observations of the variations of Fe  $K_\alpha$  line for two Seyfert 1 galaxies, NGC 4051 and NGC 4151 (Wang et al. 1999, 2001), namely both the Fe  $K_\alpha$  flux and the line profile varied drastically, but the continuum flux stayed virtually unchanged during the same time, are difficult to explain by changes of ionization states.

A comprehensive study was carried out by Weaver et al. (2001), who investigated a dozen Seyfert 1 galaxies for possible correlation between the variations of the Fe  $K_\alpha$  line (including its intensity, centroid energy and profile) and the X-ray continuum. The variability of the  $K_\alpha$  line seems ubiquitous, but in most cases not correlated with the continuum. Particularly, in NGC 5548, the line is undetected in half of the observations with fairly strict upper limits, but whether or not the line is present does not seem to correlate with the continuum flux level. These authors noticed further that in Mkn 279, only the line-center energy of the Fe  $K_\alpha$  responded perceptibly to the changes of the continuum. This may well simply imply a dependence of the ionization state of the iron ions on the incident continuum flux, rather than a support to the photoelectric absorption-fluorescence mechanism itself. These authors concluded that the general behavior of the line bears little relation to the continuum.

Another possible difficulty with the fluorescence process is that when a  $K_\alpha$  emission line is produced, there should have been a coexistent photoelectric absorption edge of the K-shell of iron ions at  $\sim 7 - 8$  KeV seen in the spectrum, as illustrated in Fig. 2 (Young et al. 1998; Ross et al. 1999; Matt et al. 1993, 1996; Fabian et al. 2000). The K-edge should be more prominent than the accompanying fluorescence Fe  $K_\alpha$  emission line because most of the absorbed K-edge photons have no contribution to the fluorescence process owing to the Auger effect. The fluorescence yield for iron ions is only  $\sim 34\%$  (Bambynek et al. 1972). However so far no conclusive evidence of the K-edge has been detected. Some authors argued that such an edge could have been diluted by the direct continuum radiation from the corona, which is stronger than the reflection component. This may well be true, but the same argument would go to the  $K_\alpha$  line itself too. The same “veiling effect” should have operated on both the absorption edge and the emission line, contradicted to what have been observed. Furthermore, the fluorescent  $K_\beta$  line of iron ions in low or intermediate ionization states has a frequency close to, and therefore would mix with, the K-edge, making the  $K_\beta$  line difficult to detect if a substantial K-drop exists. The iron  $K_\beta$  line however is distinctly seen in observations (cf Fig. 1), which argues for a K-edge shallower than that predicted by the photoabsorption-fluorescence model.

Recently Gordoin et al. (2001) claimed to have a first detection of the coexistence of the Fe  $K_\alpha$  emission line with the Fe K-edge at  $\sim 7.6$  KeV in the spectrum of Fairall 9, also a Seyfert 1

galaxy. This indeed would have lent a strong support to the fluorescence mechanism except that their quantitative fitting to the data is disappointing. In their best results, the derived optical thickness of the absorbing gas at K-edge is very small,  $\tau \approx 0.18_{-0.10}^{+0.18} \ll 1$ , even after the subtraction of the iron  $K_\beta$  emission from the observed flux. Such a small optical depth indicates that the disk is quite transparent to incident X rays, thus insufficient to produce a strong  $K_\alpha$  fluorescence line.

The complicated interplay with the  $K_\beta$  line, the reflection and dilution radiation makes the inference of the existence (or absence) of the K-edge very difficult. The lack of a *prominent* K-edge in the spectrum and the apparent absence of dependence between the continuum and the line flux prompts us to consider alternative emission mechanisms for the  $K_\alpha$  line.

### 3. The Cerenkov Line-like Radiation

We propose the “Cerenkov line-like radiation ” (You et al. 2000, 1980, 1986) as a possible mechanism for the iron emission feature in AGNs. We shall show that this emission mechanism may become predominant over the fluorescence process under certain conditions. Furthermore, both difficulties confronted by the fluorescence mechanism as mentioned above, namely the lack of correlation between the line and the continuum fluxes, and the apparent lack of coexistence of the  $K_\alpha$  line with the K-drop, can be readily alleviated because the radiation energy of Cerenkov line is provided by relativistic electrons rather than by the X-ray continuum.

The Cerenkov line-like mechanism has been confirmed by laboratory experiments in  $O_2$ ,  $Br_2$  and Na vapor using a  $^{90}Sr$   $\beta$ -ray source with the fast coincidence technique (Xu et al. 1981, 1988, 1989). Detailed discussions of its basic physics and improved formulae have been presented recently (You et al. 2000). Here we outline the physics and essential results of the theory.

When thermal relativistic electrons with isotropic distribution of velocity move in a gas region, or impinge upon the surface of a dense cloud with arbitrary shape (e.g., with spherical, filamentary or sheet-like structure), Cerenkov radiation is produced within a narrow wavelength range  $\Delta\lambda$ , very close to the intrinsic atomic or molecular wavelength  $\lambda_{lu}$ , where  $l$  and  $u$  denote, respectively, the corresponding upper and lower energy levels. Only in this narrow wavelength range is the refractive index of the gas significantly larger than unity,  $n > 1$  so as to make it possible to satisfy the Cerenkov radiation condition  $n \geq \frac{c}{v} \equiv \frac{1}{\beta}$ . The emission feature therefore appears more like an atomic or molecular line than a continuum, hence the name “Cerenkov line-like radiation”, or simply “Cerenkov emission line”.

For gas medium, the dispersion curve  $n \sim \lambda$  and the resonant line-absorption curve  $\kappa \sim \lambda$  (Fig. 3) can be calculated exactly by use of the refractive index of gas  $\tilde{n}^2 - 1 = \frac{4\pi}{3} N\alpha$ , where  $\tilde{n} = n - i\kappa$  is the complex refractive index, with the real part  $n$  being the refractive index of gas, and the imaginary part  $\kappa$  being the extinction coefficient which relates to the line-absorption coefficient;  $N$  is the number density of the atomic/molecular species;  $\alpha$  is the polarizability per

atom or ion, given by quantum theory (You et al. 2000). For a very dense gas,  $n$  is large. For  $\lambda \approx \lambda_{lu}$ , the value of  $\alpha$ , and hence the value of  $n$ , becomes very large (Fig. 3).

We note that  $n > 1$  near  $\lambda \approx \lambda_{lu}$ , even when the lower energy level  $l$  is fully closed, as long as the corresponding upper level  $u$  is not completely filled. An intermediately ionized iron would be such a case, with its K-shell completely filled, but with the L-shell still with vacancies. This is in contract to the fluorescence emission which always requires to preempt a vacancy in the lower level. It is this unique property that makes it easier to produce the  $K_\alpha$  line of iron ions in intermediate-ionization states, under certain circumstances, by the Cerenkov mechanism than by the fluorescence process.

In Fig. 3 we see that a strong line-absorption occurs at  $\lambda = \lambda_{lu}$  where the Cerenkov radiation vanishes. The Cerenkov mechanism only operates in the narrow shaded region  $\lambda > \lambda_{lu}$  where the absorption approaches zero,  $\kappa_\lambda \rightarrow 0$ . The combination of absorption and emission causes the overall feature slightly redshifted, which we call ‘‘Cerenkov line redshift’’ to distinguish it from other types of redshift mechanisms (Doppler, gravitational, Compton, etc.). A typical value for the Cerenkov line redshift would be  $z \sim 10^{-3}$ , which in terms of Doppler effect would correspond to an apparent velocity of several hundred kilometers per second (You et al. 2000). As we shall discuss below, the Cerenkov line redshift plays a decisive role in the emergent flux of Cerenkov emission line.

In summary, the Cerenkov line-like emission has the following characteristics: (1) It is concentrated in a small wavelength range near the atomic or ionic intrinsic wavelength, so appears more like a line than continuum. The denser the gas, the broader the emission ‘line’ feature. (2) The line profile is asymmetric, being steep on the high energy side and flattened on the low energy side. (3) The peak of the emission feature is not exactly at  $\lambda = \lambda_{lu}$  but slightly redshifted due to line absorption. (4) The radiation would be polarized if the relativistic electrons have an anisotropic velocity distribution.

Fig. 4 shows the calculated profile of the Cerenkov  $K_\alpha$  line of  $\text{Fe}^{+21}$ . For comparison a normal line by a spontaneous transition  $n = 2 \rightarrow 1$  of  $\text{Fe}^{+21}$  ion is also shown. The differences are obvious.

The redshift effect (item 3 above) conveniently provides a mechanism in favor of the emergence of Cerenkov line radiation, particularly from dense clouds. The absorption mechanism for a Cerenkov line is distinctly different from that for a normal line. A normal spectral line, located exactly at  $\lambda = \lambda_{lu}$ , would be greatly weakened by a strong resonance absorption because the line absorption coefficient  $k_{lu}(\lambda = \lambda_{lu})$  becomes very large (Fig. 3). In case of a very dense gas, the emergent radiation simply becomes a black-body continuum, and the normal line vanishes. In contrast, a Cerenkov line occurs at  $\lambda > \lambda_{lu}$  because of the Cerenkov redshift, so can avoid the strong line absorption,  $k_{lu}(\lambda > \lambda_{lu}) \rightarrow 0$  (Fig. 3). Therefore a Cerenkov line suffers only very small amounts of photoelectric absorption. For the Cerenkov iron  $K_\alpha$  line, the dominant photoelectric absorption comes from the L-shell electrons of iron ions,  $k_{\text{bf}}$ , which is much smaller than the regular line absorption,  $k_{lu}(\lambda_{lu})$ . That is,  $k_{\text{bf}}(\text{Fe} - \text{L}) \ll k_{lu}(\lambda = \lambda_{lu})$ . This means that

the photons of Cerenkov line can escape readily from deep inside a dense gas cloud, therefore the Cerenkov emission layer at the surface of a dense cloud would be much thicker than that of a normal line. In other words, a dense gas would appear more “transparent” for the Cerenkov line emission than for a normal line produced by the spontaneous transition. A thick emission layer at the surface of an opaque dense cloud means a possibility of very strong emergent Cerenkov line emission, predominant over the markedly weakened normal fluorescence line, as long as there are sufficient number of relativistic electrons near the surface.

#### 4. Model consideration and model calculation

As mentioned above, the Cerenkov line-like radiation may be particularly prominent in astrophysical environments with very high gas concentration and abundant relativistic electrons. One such example would be AGNs, particularly the Seyfert 1 galaxies for which existence of dense gas regions seems plausible. The gas at the surface of an AGN disk is thought to be compressed to very high density by the high radiation pressure of the coronal X rays. The validity of the disk model is not without defiance (Sulentic et al. 1998a; 1998b), and such a disk-type geometry is not required in, though it is well compatible with, the proposed Cerenkov mechanism. We therefore adopt a quasi-spherical distribution of dense cloudlets with spherical, filamentary or sheet-like shapes around the central black hole. The possible presence of such dense cloudlets, filaments and sheets in AGN environments has been discussed by Rees (1987); Celotti, Fabian & Rees (1992); Kuncic, Blackman & Rees (1996); Kuncic, Celotti & Rees (1997) and Malzac (2001). The clouds must be very dense to remain cool, and therefore held, by magnetic fields. Cool gas trapped by the magnetic field is compressed to extreme densities by the high radiation pressure, as what happens at the surface of disk surrounding the central supermassive black hole. Recently some authors propose a quasi-spherical distribution of dense clouds to explain the origin and profile of the iron  $K_{\alpha}$  line (Karas et al. 2001; Collin-Souffrin et al. 1996; Brandt et al. 2000). In their scenario, the innermost part of the disk is disrupted due to disk instabilities. Part of the disrupted material forms the optically thick, cold cloudlets of dense gas that cover a significant portion of the sky from the point of view of the central X-ray source (Boller et al. 2002), while the rest gets heated up to high temperatures, forming a corona (see Fig. 5). Recent observations support the existence of dense clouds or filaments in AGNs (Boller et al. 2002) which strongly favors the operation of Cerenkov line-like radiation mechanism.

Fig. 5 sketches the schematic of our working model of a quasi-spherical emission region around the central supermassive black hole of AGN. In the figure the blue spots or stripes represent cool cloudlets or filaments of dense gas. The yellow-dotted region stands for the hot and rarefied corona. The yellow dots represent thermal electrons and the red dots the relativistic electrons distributed nonuniformly in the corona due to the trapping by the magnetic field around the clouds.

Evidence also seems to be mounting on the existence of abundant relativistic electrons. It

is likely that the observed power-law continuum over a very wide frequency range, from radio to X rays is largely attributed to nonthermal radiation of relativistic electrons. Although the detail mechanism to produce an excessive amount of high energy electrons remains unclear, flare events or some shock processes in the corona may be responsible. Such shock processes also take place in the gamma-ray burst events, in which ultra-fast electrons are produced by internal and external shock waves (Piran 1999; Meszaros 2002). Given the ubiquity of shock events in the corona around the central supermassive black hole, and their frequent collisions with dense clouds, the whole region of the iron line emission can be regarded as a shock-filled X-ray source (Fig. 5). The collisions convert part of the kinetic energy of shock wave to thermal energy of relativistic electrons (Piran 1999). Most fast electrons thus produced are concentrated in a narrow zone close to the collision front at the surface of the dense cloudlet (or on the flare spots if they are produced in flare events), as shown in Fig. 5. Diffusion of fast electrons outward to ambient space is hampered by to the trapping effect of magnetic fields near the clouds or flares. The ability to retain extremely high concentration of relativistic electrons near the surfaces of dense clouds undoubtedly provides a very favorable environment for the operation of the Cerenkov line emission.

If the conditions, namely the existence of dense gas and relativistic electrons, are met, the Cerenkov line like emission becomes inevitable. We now derive the luminosity of the Cerenkov Fe  $K_\alpha$  line under various environmental parameters, and compare it with observations. The main factors that determine the luminosity of the Cerenkov line, in addition to the geometric size of the line emitting region, include the density of the iron ions  $N_{\text{Fe}}$ , the density of the relativistic electrons  $N_e$ , and the average energy  $\gamma_c$  of the relativistic electrons, where the Lorentz factor  $\gamma \equiv \frac{1}{\sqrt{1-\beta^2}} = \frac{mc^2}{m_0c^2}$  represents the dimensionless energy of an electron in unit of  $m_0c^2$ . Our goal is to estimate the (range of ) values of  $N_e$ ,  $N_{\text{Fe}}$  and  $\gamma_c$  from the theory of Cerenkov line radiation (You et al. 2000), to match the observed luminosities of the Fe  $K_\alpha$  line, and in turn to see whether these values are acceptable in the environment of AGNs.

In this paper, our main interest is in the energetics of the Fe  $K_\alpha$  emission process, therefore we leave out lengthy discussion on the line profile, except to note that even though a Cerenkov line is intrinsically broad, asymmetric, and redshifted, it is still insufficient to produce the highly skew Fe  $K_\alpha$  line observed in AGNs. A supermassive black hole is still needed to provide the necessary Doppler broadening and gravitational redshift.

We assume a mass  $M \sim 10^{7-8}M_\odot$  for the central black hole. From the observed variation time scales of the Fe  $K_\alpha$  line ( $\sim 1$  lt day, see Nandra, Mushotzky, et al. 2000 ?????????), we infer the size of the emission region to be  $D \sim 10^{15-16}$ cm. In the following calculations, we adopt a typical value  $D \approx 3 \times 10^{15}$ cm, or about  $\sim 10^{2-3}R_{\text{Sch}}$ , where  $R_{\text{Sch}}$  is the Schwarzschild radius. To simplify the calculation, we assume all the dense gas in the form of spherical cloudlets with the same radius, except to note that in reality they will naturally be in various cloud-like, filament-like or sheet-like shapes with various sizes. As noted before, because of the strong irradiation from the central X-ray source, there should exist a photoionized layer at the surface of a cloudlet. The main species of the iron ions in this layer should be in intermediate-ionization states, e.g., those

from  $\text{Fe}^{+18}$  to  $\sim \text{Fe}^{+21}$ , because in many cases the observed line centers are around 6.47–6.5 KeV (e.g., Wang et al. 1998; Weaver et al. 2001). Denoting the total number of cloudlets in the whole emission region as  $\tilde{N}$ , and the radius of each cloudlet as  $r$ , the covering factor of cloudlets to the central X-ray source is

$$f_c = \frac{\tilde{N}\pi r^2}{4\pi D^2} = \frac{\tilde{N}r^2}{4D^2}$$

, which must be less than unity to ensure the central X-ray source to be only partly covered. We see that the unknown quantity  $\tilde{N}r^2$  can be removed by  $f_c$  and  $D$ . The volume filling factor is

$$f_v = \frac{\tilde{N}4\pi r^3/3}{4\pi D^3/3} = \tilde{N} \frac{r^3}{D^3}. \quad (1)$$

Therefore the ratio is  $f_v/f_c \approx r/D$ , which means that the fractional volume occupied by the clouds would be very small if  $r \ll D$ . At the same time,  $\tilde{N}$  can still be very large to maintain a necessarily large covering factor  $f_c$ .

The emergent intensity of Cerenkov Fe  $K_\alpha$  line from the surface of dense cloud is (Eq.(42) in You et al. 2000)

$$I_{K_\alpha}^c = Y \left[ \ln(1 + X^2) - 2 \left( 1 - \frac{\arctan X}{X} \right) \right] \quad (\text{ergs/Sec.} \cdot \text{cm}^2 \cdot \text{Str.}), \quad (2)$$

where the parameter  $Y \equiv \frac{N_e C_1}{2k_{\text{bf}}} \propto N_e$ , the density of relativistic electrons; and  $X \equiv \sqrt{\frac{k_{\text{bf}}}{C_2}} C_0 \gamma_c^2 \propto \gamma_c^2 N_{\text{Fe}}$ , where  $N_{\text{Fe}}$  and  $\gamma_c$  represent, respectively, the density of iron ions in gas cloudlets and the typical energy of the relativistic electrons;  $C_0$ ,  $C_1$ ,  $C_2$  and  $k_{\text{bf}}$  included in  $X$  and  $Y$ , are the parameters dependent on the density  $N_{\text{Fe}}$  and the atomic parameters of concerned ions, e.g., the frequency  $\nu_{lu}$  (or  $h\nu_{lu} \equiv \varepsilon_{lu}$ ), the transition probability  $A_{ul}$ , etc. (see Eq.(32') in You et al. 2000). Inserting the concerned atomic parameters of the iron ions, we obtain<sup>1</sup>

$$\begin{aligned} X &\equiv \sqrt{\frac{k_{\text{bf}}}{C_2}} C_0 \gamma_c^2 = 6.4868 \times 10^{-28} g_2 \sqrt{\frac{S_2}{g_2} \left( \frac{S_1}{g_1} - \frac{S_2}{g_2} \right)} N_{\text{Fe}} \gamma_c^2, \\ Y &\equiv \frac{N_e C_1}{2k_{\text{bf}}} = 0.1632 \times \frac{g_2}{S_2} \left( \frac{S_1}{g_1} - \frac{S_2}{g_2} \right) N_e, \end{aligned} \quad (3)$$

where  $g_2$  and  $S_2$  represent respectively the degeneracy and the real occupation number of electrons for the second level of the iron ion, so  $S_2 \leq g_2$ ;  $g_1$  and  $S_1$  are the corresponding quantities for the first level.

---

<sup>1</sup>The CGSE system of units is used throughout in our original paper (You et al. 2000). This means, in particular, that all wavelengths in optical bands would be in centimeters rather than in Å. The photon energy in X-ray bands would be in ergs rather than KeV. For the  $\text{Fe}^{+16}$   $K_\alpha$  line, the photon energy in related Cerenkov formulae is  $\varepsilon_{lu} \equiv \varepsilon_{21} = 6.45 \text{ KeV} = 1.03 \times 10^{-8} \text{ erg}$ , rather than 6.45 KeV.



From Eq. (4) we see that in a physically reasonable environment in AGNs, it usually holds that  $X \ll 1$ . Therefore Eq.(3) is simplified as

$$I_{K_\alpha}^c \approx Y X^2/3, \quad (4)$$

The Cerenkov line emission produced by thermal relativistic electrons with random direction-distribution of velocity is isotropic, thus the Cerenkov intensity  $I_{K_\alpha}^c$  is  $\theta$ -independent. Therefore the emergent flux  $F_{K_\alpha}^c$  from the surface of dense cloud is simply obtained

$$F_{K_\alpha}^c = 2\pi \int_0^{\pi/2} I_{K_\alpha}^c \cos \theta \sin \theta d\theta = \pi I_{K_\alpha}^c \quad (\text{ergs/Sec.} \cdot \text{cm}^2). \quad (5)$$

So the elementary luminosity of the Cerenkov Fe  $K_\alpha$  line of each cloudlet is

$$l_{K_\alpha}^c = 4\pi r^2 F_{K_\alpha}^c = 4\pi^2 r^2 I_{K_\alpha}^c \quad (\text{ergs/Sec.}). \quad (6)$$

Combining Eq.(1) and (7), the total luminosity of Cerenkov Fe  $K_\alpha$  line from the whole emission region becomes

$$L_{K_\alpha}^c = \tilde{N} l_{K_\alpha}^c = 4\pi^2 r^2 \tilde{N} I_{K_\alpha}^c \approx 16\pi^2 D^2 f_c I_{K_\alpha}^c \quad (\text{ergs/Sec.}). \quad (7)$$

Inserting Eq. (4) and (5) into (8), taking  $D \approx 3 \times 10^{15}$  cm and  $f_c \approx 0.1$ , and  $S_1 = g_1 = 2$ , we obtain

$$L_{K_\alpha}^c = 2.0821 \times 10^{-22} \left(1 - \frac{S_2}{g_2}\right)^2 N_e N_{Fe}^2 \gamma_c^4 \quad (\text{ergs/Sec.}), \quad (8)$$

Comparing the luminosity of Cerenkov Fe  $K_\alpha$  line Eq. (9) with the typical observed value for Seyfert 1 galaxies, i.e.,  $L_{K_\alpha}^{\text{obs.}} \approx 10^{40-41}$  ergs/Sec., letting  $L_{K_\alpha}^c \approx L_{K_\alpha}^{\text{obs.}}$ , we obtain

$$N_{Fe}^2 \gamma_c^4 N_e \approx 4.8 \times 10^{61} \left(1 - \frac{S_2}{g_2}\right)^{-2} \approx 10^{62}, \quad (9)$$

where for intermediate-ionization iron ions, we take  $S_2 \approx 1 - 5$ . Eq.(10) gives the condition for the iron density  $N_{Fe}$ , the density of fast electrons  $N_e$ , and the average or typical energy  $\gamma_c$  of the fast electrons to produce the observed luminosity of the Fe  $K_\alpha$  line.

Table 1 lists several tentative sets of parameters under the condition, where we arbitrarily fix  $N_e = 10^{10}$  cm<sup>-3</sup>. The choice of combinations is somewhat arbitrary, because so far the environments in AGNs are not well understood. Some of these parameters may at first appear defiant to the current paradigm around AGN black holes. In the following section we give discussions on the reasonableness and acceptability of these parameters and the related new scenario around the supermassive black hole in AGNs.

## 5. Discussions and Conclusions

?? We tentatively propose another mechanism—the ‘Cerenkov line like radiation’ — to study the origin of the elusive Fe  $K_\alpha$  feature in AGNs. The charming advantage of this new emission mechanism is that the radiation energy of the Cerenkov line is provided by the relativistic electrons rather than by the X-ray continuum. Therefore the continuum and the Fe  $K_\alpha$  line emission are two components independent of each other. So the lack of coexistence of Fe  $K_\alpha$  line with the K-edge and the lack of correlation between the line and the continuum fluxes in observations can be understood by this way. We further give some model calculations to show the effectiveness of the Cerenkov mechanism to explain the AGNs observations. We show that the calculated Cerenkov Fe  $K_\alpha$  is strong enough to compare with the observed line-luminosity of AGNs, only if the iron density of the dense gas  $N_{\text{Fe}}$ , the density of fast electrons  $N_e$  and the characteristic energy of fast electrons  $\gamma_c$  are high enough, as shown in Table.1.

??? If the Fe  $K_\alpha$  feature indeed arises from the Cerenkov line mechanism, Table.1 signifies the possibility of a strikingly different scenario around the supermassive black hole in AGNs—with much denser, more violent and energetic environs than conventionally believed.

Therefore we must make a serious check on the possibility and reasonableness of the new scenario. Firstly, what are the consequences if there exist abundant relativistic electrons with exceedingly high energies? In fact, in addition to the Cerenkov line radiation, fast electrons also contribute substantially to the continuum radiation through inverse Compton scattering (the synchrotron process does not operate in a very dense gas). The Compton power of a fast electron with energy  $\gamma_c$ , passing through a radiation field of X rays with an energy density  $U_{\text{ph}}$  is  $p^{\text{Comp}} \approx 2.6 \times 10^{-14} U_{\text{ph}} \gamma_c^2 \approx 10^{-15} \gamma_c^2$  ( $U_{\text{ph}} \approx 0.1$  ergs/cm<sup>3</sup> for typical Seyfert 1 galaxies). If the density and energy of the fast electrons are so high as  $N_e \approx 10^9\text{--}10^{10}$  cm<sup>-3</sup>, and  $\gamma_c \approx 10^{4\text{--}5}$ , as shown in Table 1, the Compton luminosity of the continuum in the whole emission region with size  $D \sim 10^{15}$  cm would be unacceptably higher than the typical observed value  $L \approx 10^{44}$  ergs/s. Another related problem is that, if the fast electrons responsible for the Fe K-line emission also have a significant contribution to the X-ray continuum from the inverse Compton scattering, i.e., Fe  $K_\alpha$  line emission and significant portion of the continuum both originate from the same group of fast electrons, then the Fe  $K_\alpha$  line flux and the continuum flux would be expected to correlate again, as in the case of photoelectric absorption-fluorescence model.

We would argue, however, that these two difficulties can be overcome if the fractional volume occupied by the cloudlets, where most fast electrons reside, is very small compared to the overall volume of the X-ray emitting region, i.e., if  $f_v \ll 1$ . In this case, the total number of fast electrons need not be very large, thus the corresponding Compton luminosity of the continuum  $L^{\text{Comp}} \approx f_v \left(\frac{4\pi}{3} D^3\right) N_e p^{\text{Comp}}$  would be several orders lower than the typical value of the observed continuum luminosity  $L \approx 10^{43\text{--}44}$  ergs/Sec.. A small  $f_v$  with a large  $f_c$  can be realized as long as  $r \ll D$ , as mentioned above. For example, taking  $D \sim 10^{15}$  cm,  $r \sim 10^{6\text{--}7}$  cm, and  $f_c \sim 0.1$ , then the filling factor is small as  $f_v \sim 10^{-10} - 10^{-9}$ , hence we get  $L^{\text{Comp}} \ll L^{\text{obs}} \sim 10^{44}$  ergs/s.

Another potential problem concerns the very high gas density. If  $N_{\text{Fe}}$  is as high as those shown in Table 1, up to  $\sim 10^{17-18} \text{ cm}^{-3}$ , and if a cosmological abundance in AGNs is assumed, then the inferred gas density would be inconceivably high. To restrict the total gas density at an acceptable level, we envisage two possibilities: either frequent nuclear reactions in the vicinity of the central black hole or a phase transition in dense gas to form dusty clouds, could be responsible for the increase of abundance of iron and other heavy elements without enhancement of the total gas density. In the latter case, the iron ions may be locked up in tiny grains as embedded impurity. A high density of impurity iron is achievable in heavily doped solids, possibly even as high as  $N_{\text{Fe}} \sim 10^{17-18} \text{ cm}^{-3}$ . It is conceivable, in principle, that the Cerenkov line-like radiation of iron ions may also occur in the impurity-doped dust, as in gas medium. Undoubtedly, the Cerenkov line-like radiation from impurity-doped solid would be a challenging problem in experimental physics. Existence of dusty clouds with iron-doped grains in the environments of AGNs would be equally mind-boggling in black hole physics.

The work of JHY is supported by the Natural Science Foundation of China, grant No. 19773005. WPC acknowledges the grant NSC91-2112-M-008-043 from the National Science Council.

## REFERENCES

- Bambynek W., et al., 1972, *Rev. Mod. Phys.*, 44, 716
- Boller Th., Fabian A. C., Sunyaev R., Trumper J., Vaughan S., Ballantyne D. R., 2002, *MNRAS*, 329, 1
- Brandt W. N., Gallagher S. C., 2000, *New Astronomy Reviews*, 44, 461
- Celotti A., Fabian A. C., Rees M. J., 1992, *MNRAS*, 255, 419
- Chiang J., et al., 2000, *ApJ*, 528, 292
- Collin-Souffrin S., Czerny B., Dumont A. M., Zycki P. T., 1996, *A&A*, 314, 393
- Fabian A. C., Rees M. J., Stella L., White N. E., 1989, *MNRAS*, 238, 729
- Fabian A. C., Vaughan S., Nandra K., Iwasawa K., Ballantyne D. R., Lee J. C., De Rosa, A., Turner A., Young A. J., 2002, *MNRAS*, 335, L1
- Gordoin P., Lumb D., Siddiqui H., Guainazzi M., Schartel N., 2001, *A&A*, 373, 805
- Guilbert P. W., Rees M. J., 1998, *MNRAS*, 233, 475
- Karas V., Czerny B., Abrassart A., Abramowicz M. A., 2000, *MNRAS*, 318, 547
- Kuncic Z., Blackman E. G., Rees M. J., 1996, *MNRAS*, 283, 1322
- Kuncic Z., Celotti A., Rees M. J., 1997, *MNRAS*, 284, 717
- Lee J., Fabian A. C., Brandt W. N., Reynolds C. S., Iwasawa K., 1999, *MNRAS*, 310, 973
- Lee J., Fabian A. C., Reynolds C. S., Brandt W. N., Iwasawa K., 2000, *MNRAS*, 318, 857
- Lightman A. P., White T. R., 1998, *ApJ*, 335, 57
- Malzac J., 2001, *MNRAS*, 325, 1625
- Matt G., Fabian A. C., Ross R. R., 1993, *MNRAS*, 262, 179; 1996, *MNRAS*, 280, 823
- Meszáros, P., 2002, *ARA&A*, 40, 137
- Nandra K., George I. M., Mushotzky R. F., Turner T. J., Yaqoob T., 1997a, *ApJ*, 477, 602; 1997b, *ApJ*, 488, 91
- Piran T., 1999, *Physics Reports*, 314, 575
- Rees M. J., 1987, *MNRAS*, 228, 47
- Reynolds C. S., 2001, *ASP Conf. Series Vol. TBD*, p105

- Ross R. R., Fabian A. C., Young A. J., 1999, MNRAS, 306, 461
- Sulentic J. W., Marziani P., Calvani M., 1998a, ApJ, 497, L65
- Sulentic J. W., Marziani P., Zwitter T., Calvani M., Dultzin-Hacyan D., 1998b, ApJ, 501, 54
- Tanaka, Y et al., 1995, Nature, 375, 659
- Wang T. G., Otani C., Cappi M., Leighly K. M., Brinkmann W., Matsuoka M., 1998, MNRAS, 293, 397
- Wang J. X., Wang T. G., Zhou Y. Y., 2001, ApJ, 549, 891
- Wang J. X., Zhou Y. Y., Xu H. G., Wang T. G., 1999, ApJ, 516, 65
- Weaver K. A., Gelbord J., Yaqoob T., 2001 ApJ, 550, 261
- Xu K., Z., Yang B. X., Xi F. Y., 1981, Phys. Lett. A86, 24
- Xu K., Z., Yang B. X., Xi F. Y., 1988, Phys. Rev. A33, 2912
- Xu K., Z., Yang B. X., Xi F. Y., 1989, Phys. Rev. A40, 5411
- You J. H., Xu Y. D., Liu D. B., Shi J. R., Jin G. X., 2000, A&A, 362, 762
- You J. H., Cheng F. H., 1980, Acta Phys. Sinica, 29, 927
- You J. H., Cheng F. H., Cheng F. Z., Kiang T., 1986, Phys. Rev. A34, 3015
- Young A. J., Ross R. R., Fabian A. C., 1998, MNRAS, 300, 11

Table 1: Combinations of Iron Density, Characteristic Energy and Density of Relativistic Electrons for Calculation of Cerenkov Luminosity of Iron  $K_\alpha$  Line

$N_{Fe}(\text{cm}^{-3})$	$\gamma_c$	$N_e(\text{cm}^{-3})$
$10^{14}$	$10^6$	$10^{10}$
$10^{15}$	$3 \times 10^5$	$10^{10}$
$10^{16}$	$10^5$	$10^{10}$
$10^{17}$	$3 \times 10^4$	$10^{10}$
$10^{18}$	$10^4$	$10^{10}$

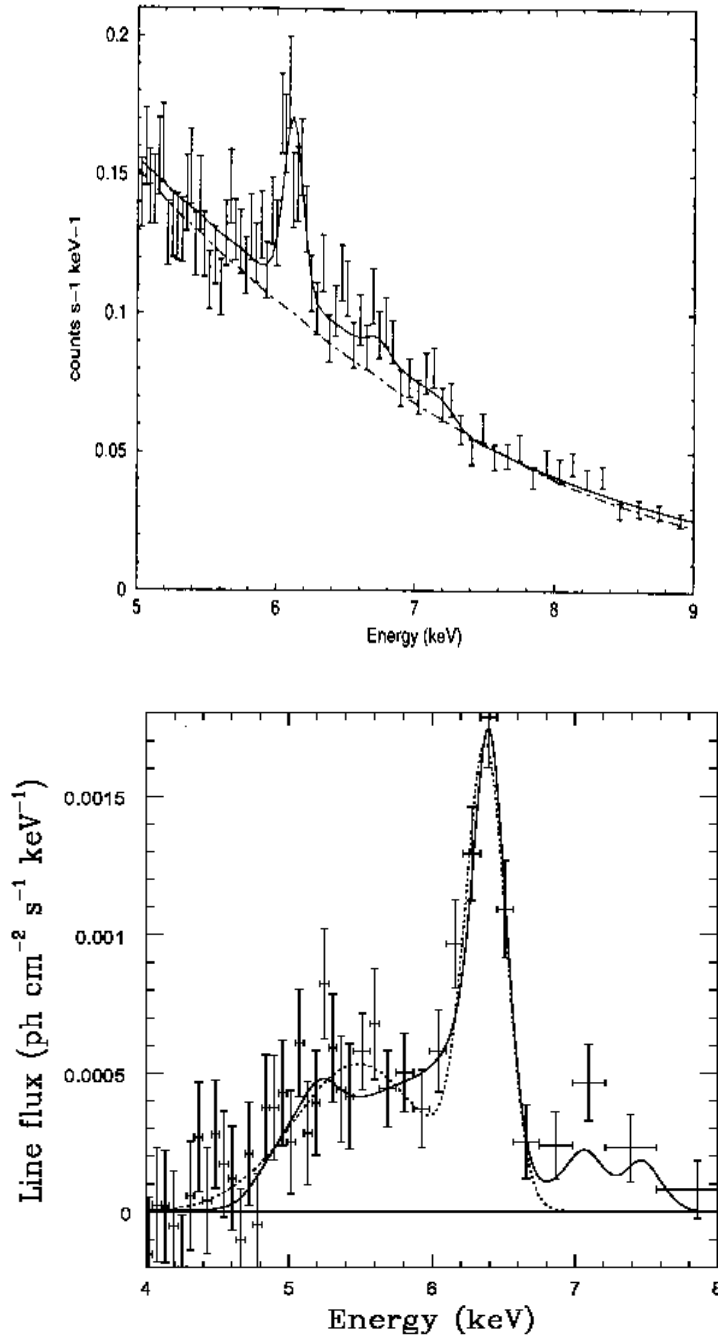


Fig. 1.— The observed Fe  $K_{\alpha}$  line of Seyfert 1 galaxy Fairall 9 (upper panel, taken from Gordin et al. 2001) and MCG-6-30-15 (lower panel, taken from Fabian et al. 2002). The small line-like hump at  $\sim 7 - 8$ KeV (in rest frame) is due to the Fe  $K_{\beta}$  line emission.

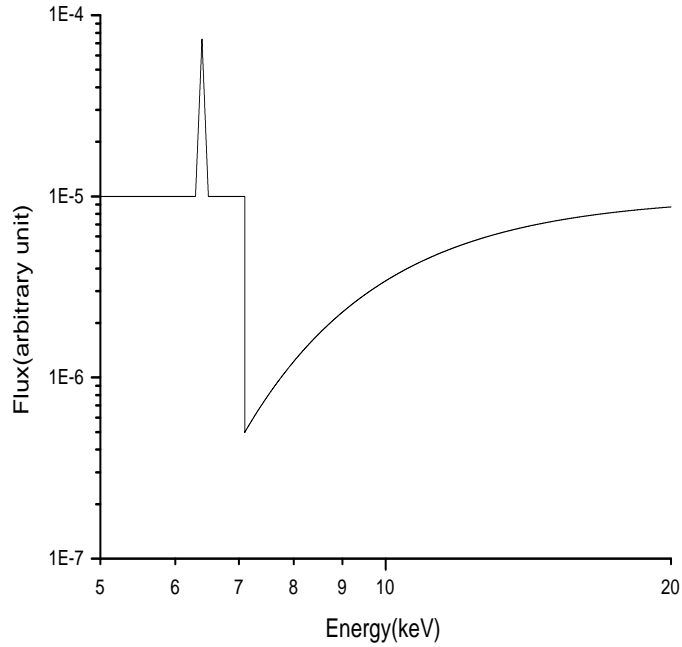


Fig. 2.— The simple spectrum of K-absorption edge or drop at  $\sim 7 - 8\text{KeV}$  in X-ray continuum, originating from photoelectric absorption of electrons in the ground state of iron ions in low- or intermediate-ionization states. Fig. 2 shows schematically the coexistence of the iron  $K_{\alpha}$  emission line and the K-absorption edge for a dense gas irradiated by X-ray continuum.



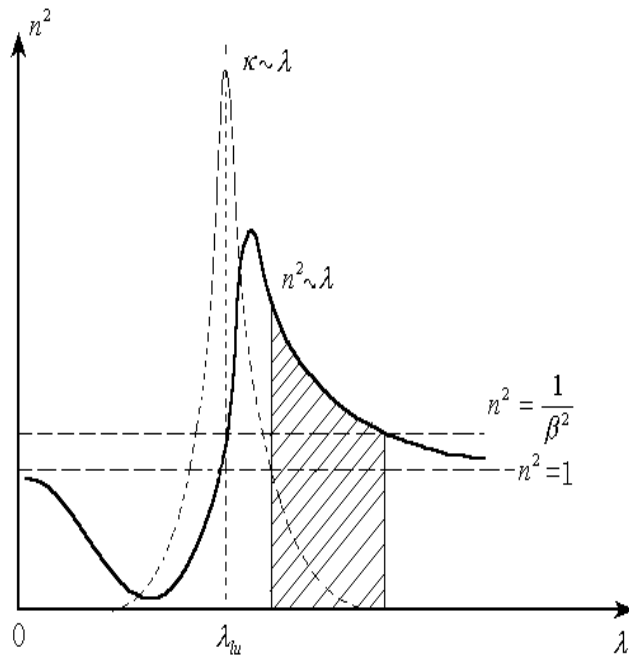


Fig. 3.— Relation between refractive index  $n$  and wavelength  $\lambda$ , and relation between extinction coefficient  $\kappa$  and wavelength  $\lambda$  (You et al. 1986). The Cerenkov radiation survives in the shaded narrow region where the Cerenkov radiation condition  $n \geq 1/\beta$  is satisfied, and where the extinction is small. The shaded region is narrow, making the emerging radiation appear more like a line emission than a continuum.

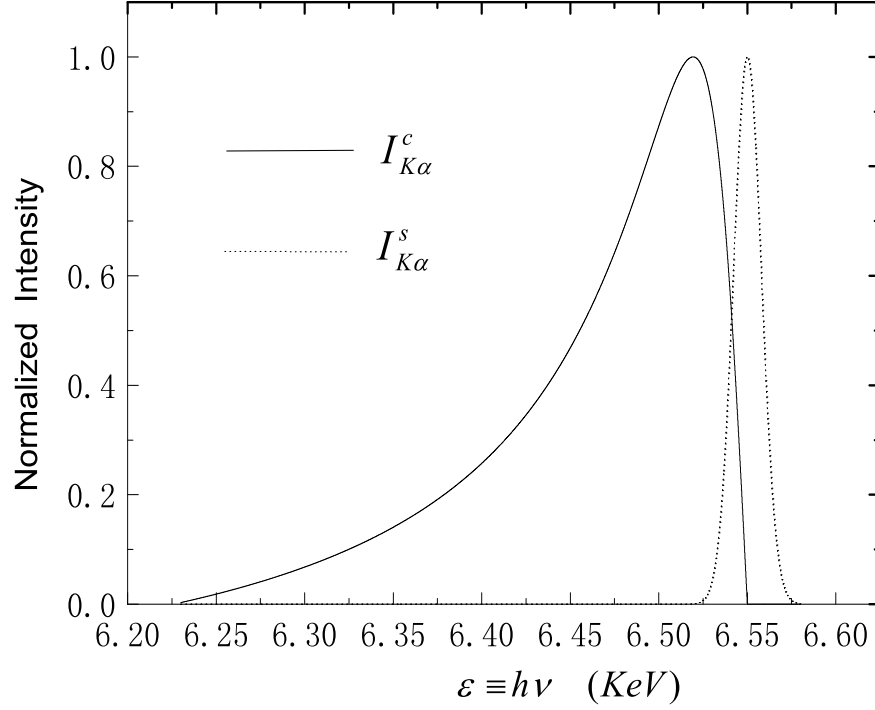


Fig. 4.— The calculated profile of Cerenkov line  $I_{K\alpha}^c \sim \varepsilon$  of iron ion  $\text{Fe}^{+21}$ , assuming  $N_{Fe} = 10^{17} \text{cm}^{-3}$  and  $\gamma_c = 2 \times 10^5$ , where  $\varepsilon \equiv h\nu$  is the energy of line photon. The Cerenkov line-profile is broad, asymmetric, and redshifted. A normal line by spontaneous transition  $I_{K\alpha}^s \sim \varepsilon$  is plotted for comparison.

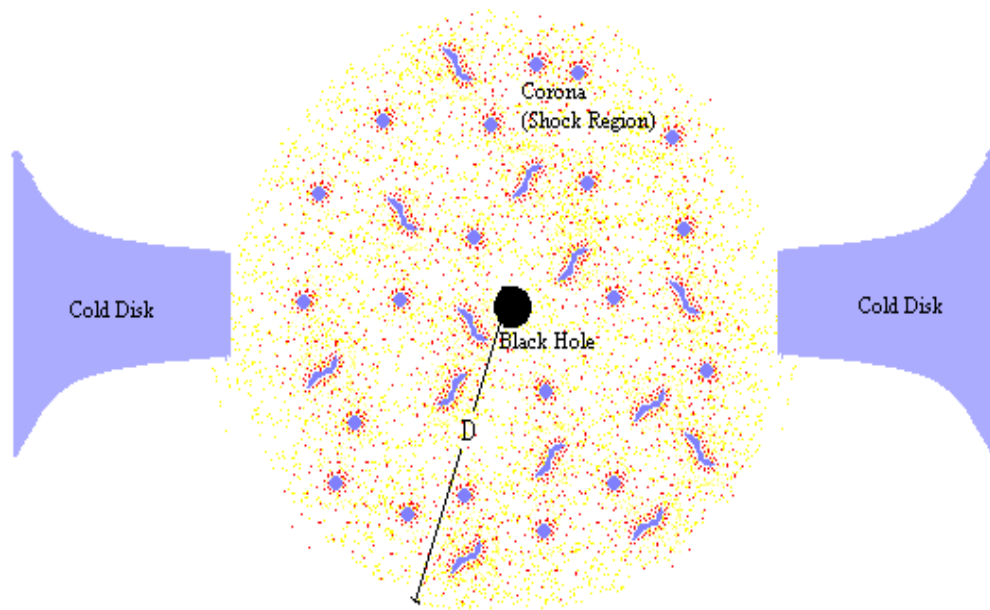


Fig. 5.— Schematic sketch of the emission region of iron  $K_\alpha$  line around a central supermassive black hole of AGN. The blue spots or strips represent cloudlets or filaments consist of cold dense gas. The yellow-dotted region is the hot, rarified corona where the yellow dots and red dots represent thermal electrons and relativistic electrons respectively.